Compensated thermohaline fronts

Outline

Observations (Rudnick and Ferrari, 1999) RF99

In the ocean density is given by

$$\Delta\rho \approx -\alpha\Delta T + \beta\Delta S$$

where α and β are the expansion coefficients. Temperature T and Salinity S are the two most important physical properties of seawater:

- they determine the density field at fixed pressure
- they are often used as tracers to infer the general circulation of the ocean
- Iselin(1939) first noticed the correspondence between horizontal profiles in the surface Mixed Layer (ML) and vertical profiles in the thermocline, and concluded that subsurface water is derived from late winter surface water. Properties set in the winter ML remain essentially unchanged during subduction and thus the T/S relationship is established in the surface ML.

A measure of the relative effects of temperature and salinity on density is the density ratio defined as

$$R \equiv \frac{\alpha\Delta T}{\beta\Delta S}$$

A horizontal compensated density front (e.g. with cold and fresh water on one side and warm and salty on the other side) is such that temperature and salinity effects exactly compensate will correspond to a density ratio $R = 1$, $\Delta\rho = 0$.

High-resolution measurements in the ocean mixed layer have been performed in the North Pacific between 25°N and 35°N along 140°W using a SeaSoar, equipped with sensors to measure T, S and pressure.

A tow was made along the 50-dbar pressure surface, within the Mixed Layer with a horizontal resolution down to 4m and a vertical deviation of less than 0.3 dbar.

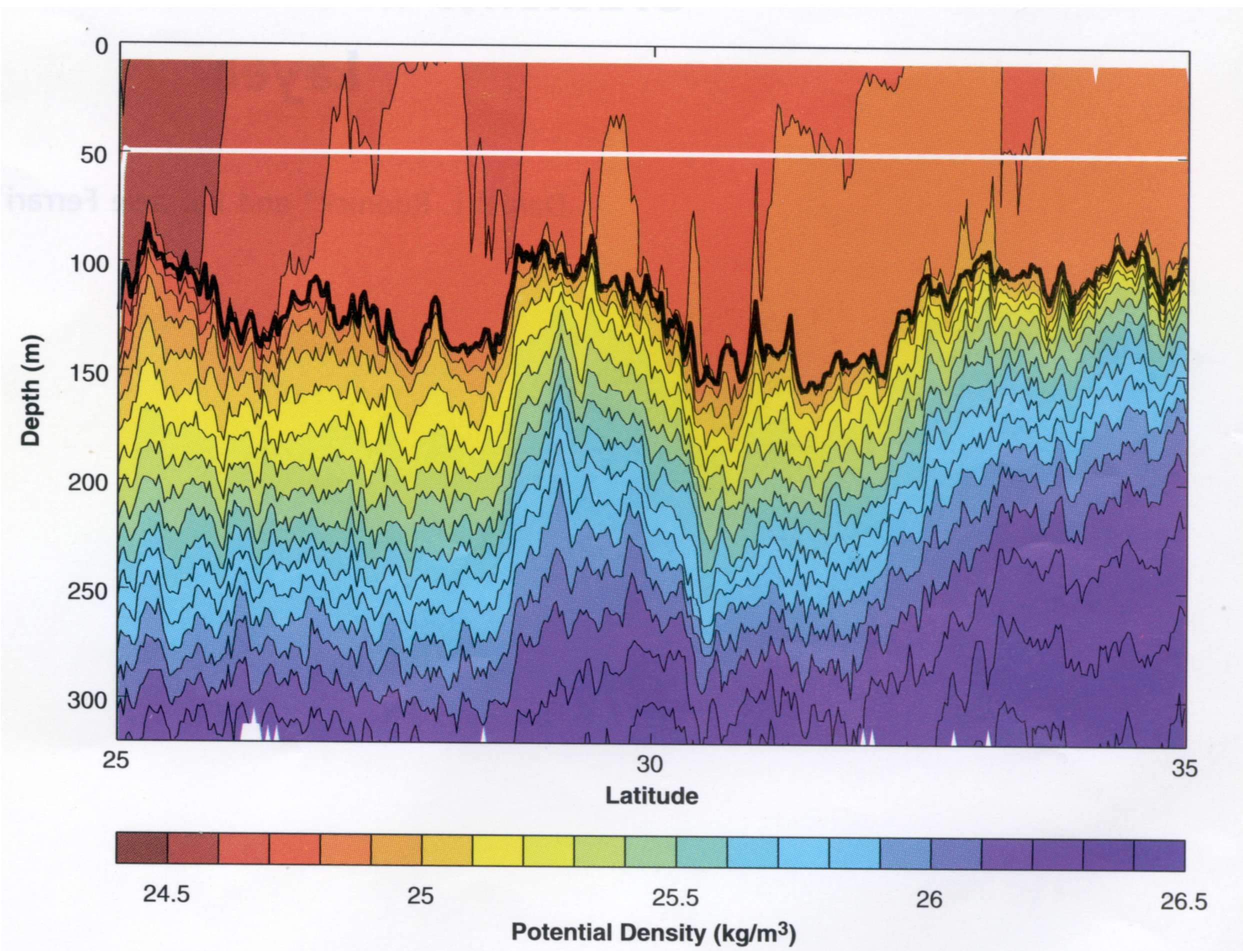

Potential density section along 140°W

Data from the 50-dbar tow demonstrate that T and S are strongly coherent over all length scales observed. Temperature and Salinity gradients coincide in such a way that density gradients are minimized: each feature in T no matter how small is mirrored in S.

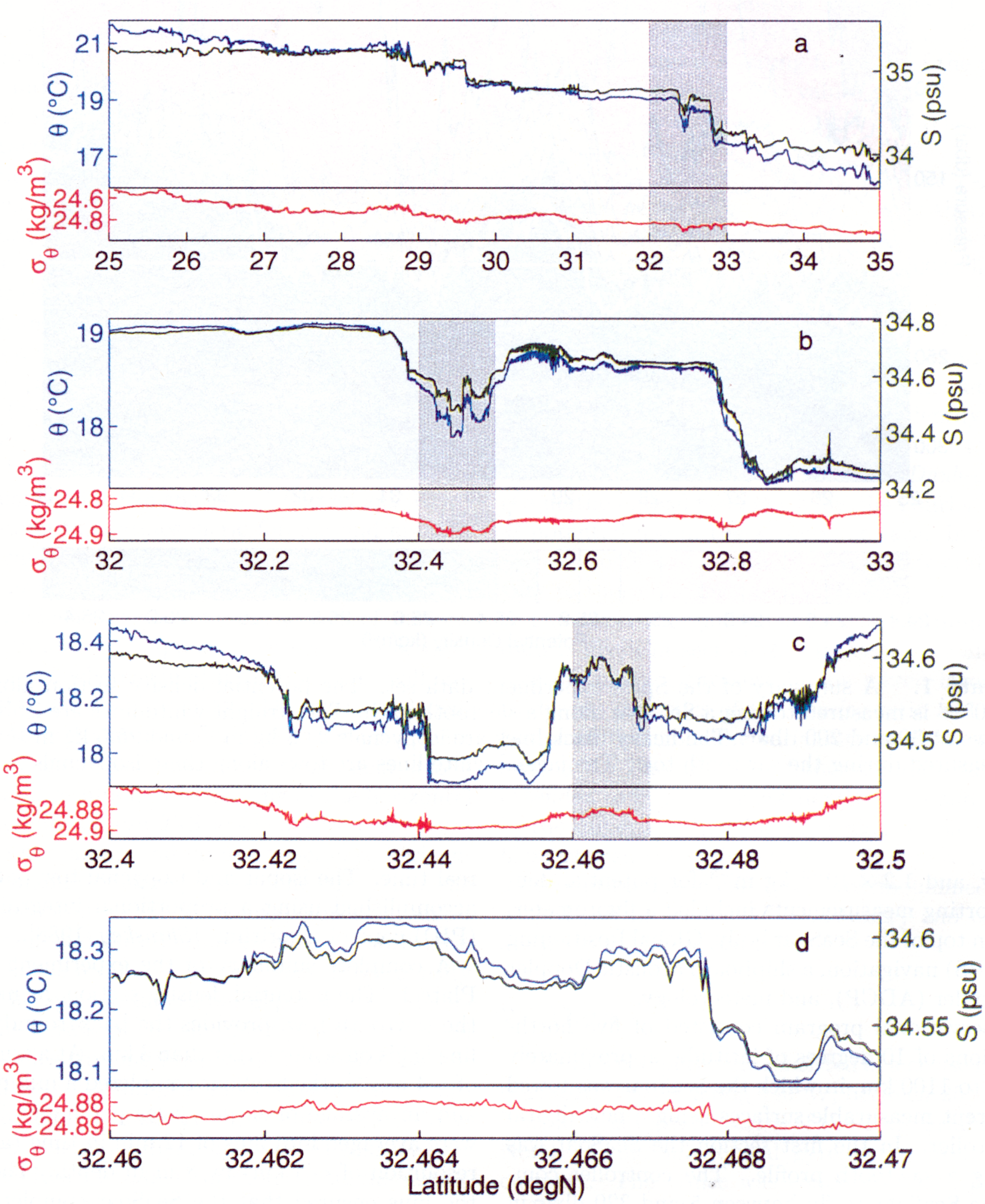

Temperature and Salinity at 50dbar.

Compensation between T and S exists at all scales in the data, and strong density gradients are rarely seen even at the smallest scales.

A wavelet transform has been used by RF99 that has the benefit to be both scale and location selective.

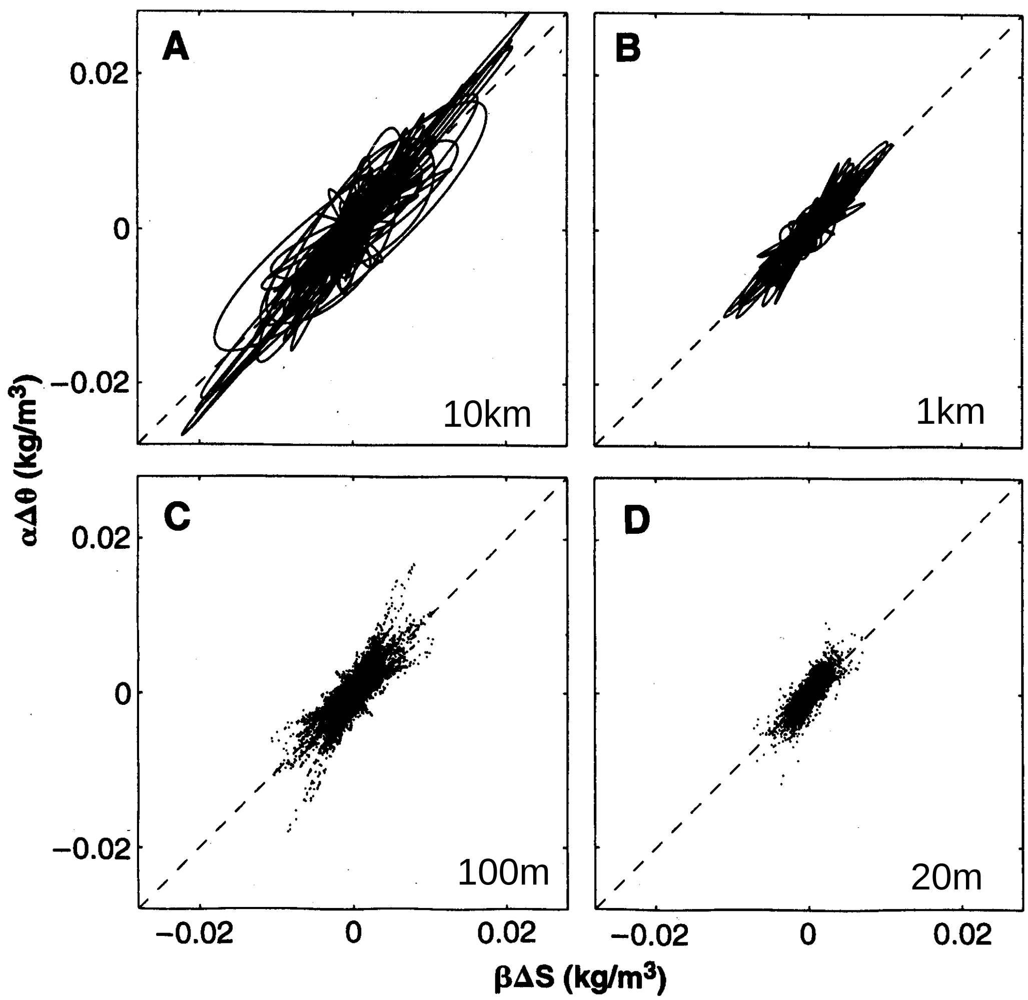

Scatterplots of wavelet coefficients of T and S for wavelengths between 20 m and 10 km

A point in the scatterplot indicates the variability of T and S at a particular wavelength and location.

The data have a slope close to 1, indicating a tendency for compensation of temperature and salinity $\Longrightarrow R = 1$

Another measure is the median ratio of the wavelet coefficients of T and S

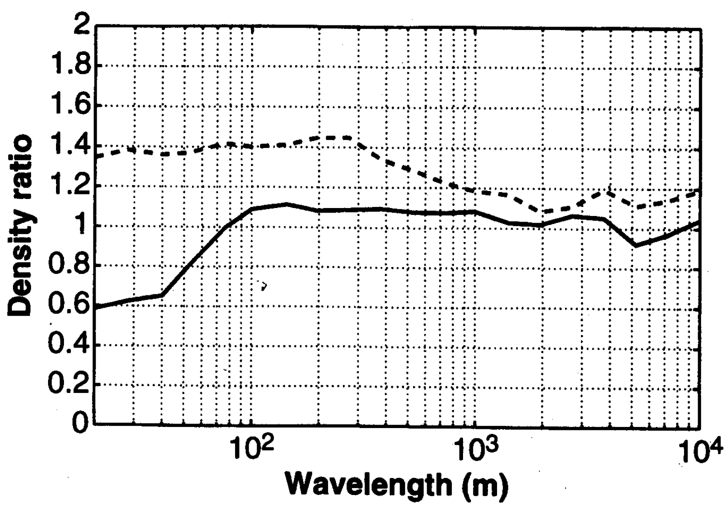

Density ratio R as a function of wavelength computed as a median (solid line) and as the slope of the principal axis

Results show that the strongest T and S fronts tend to be compensated at all scales ranging from 100 m to 10 km.
This suggests that the ML mixes horizontally in such a way that density gradients are dissipated while compensated temperature and salinity gradients persist.

Labrador Sea observations (Lilly et al. 1999)

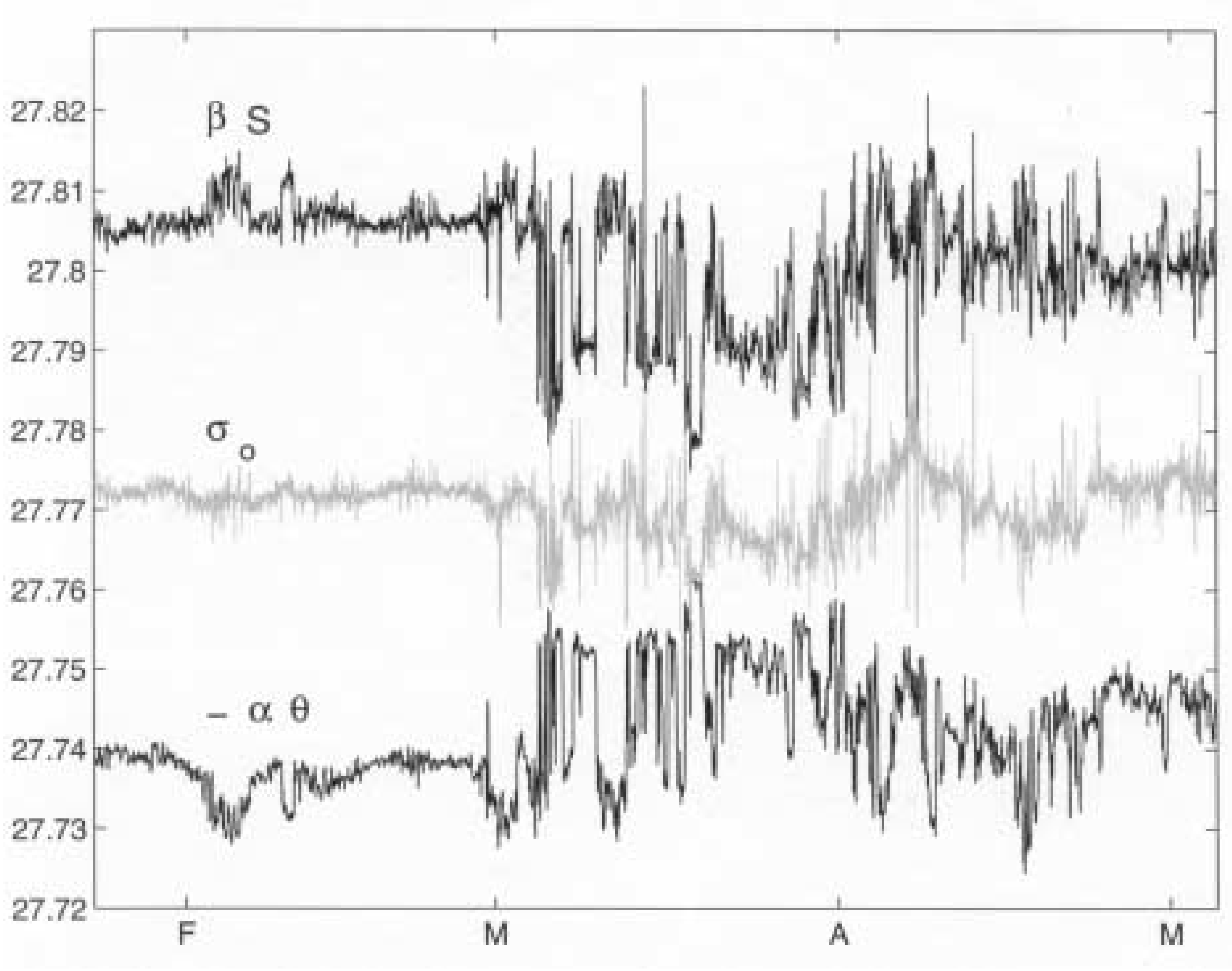

Creation of density compensated thermohaline structure by nonlinear diffusion (Ferrari & Young), FY97

Nonrotating stratified fluid which density is $\rho = \rho_0[1 - g^{-1}B(x, y, z, t)]$ where $B(x, y, z, t)$ is the buoyancy, and a linear equation of state

$$B = T - S$$

T temperature, S is the salinity. Equations of motion are

$$\begin{aligned}
\frac{D\boldsymbol{u}}{Dt} &= -\boldsymbol{\nabla}\ p + B\hat{\boldsymbol{z}} + \text{mix} \\
\boldsymbol{\nabla}\cdot\boldsymbol{u} &= 0 \\
\frac{D\ S}{Dt} &= \text{mix} \\
\frac{D\ T}{Dt} &= \text{mix}
\end{aligned}$$

where $\boldsymbol{u} = (u, v, w)$ and "mix" indicates an episodic mixing model and instantaneous homogenization of momentum and of the stratifying components.

For given initial conditions, exact solutions of this system of equations can be found which correspond simply to dense fluid slumping under lighter fluid, while the pressure gradient drives the accelerating, vertically sheared flow.

FY97 show that in this case too the average fluxes of tracers T and S can be computed, leading to the vertically-averaged heat and salt equations:

$$\begin{aligned} T_t &= \gamma \boldsymbol{\nabla} \cdot [(\boldsymbol{\nabla} B \cdot \boldsymbol{\nabla} T) \boldsymbol{\nabla} B] \\ S_t &= \gamma \boldsymbol{\nabla} \cdot [(\boldsymbol{\nabla} B \cdot \boldsymbol{\nabla} S) \boldsymbol{\nabla} B] \end{aligned}$$

with γ a dimensional factor.

Such relations correspond to a flux of tracer which is proportional to the cube of the tracer gradients.

The flux of salt is in the direction of the buoyancy gradient. This differs from eddy mixing arguments that would state that the flux of salt is parallel to the salt gradient.

In the slumping problem (and in density driven shear dispersion in general) the velocity is always in the direction of the buoyancy gradient.

By combining these two equations, the buoyancy equation becomes

$$B_t = \gamma \, \boldsymbol{\nabla} \cdot [(\boldsymbol{\nabla} B \cdot \boldsymbol{\nabla} B) \, \boldsymbol{\nabla} B]$$

Monte-Carlo simulations

Initial temperature and salinity with zero correlation, with T and S having uniform probability density function with zero mean.

Numerical simulations of the coupled equations for temperature and salinity gradients with $\gamma = 1$

$$(T_x)_t = (B_x^2 T_x)_{xx}, \quad (S_x)_t = (B_x^2 S_x)_{xx}$$

Global conservations of heat and salt by no-flux boundary conditions on T_x and S_x.

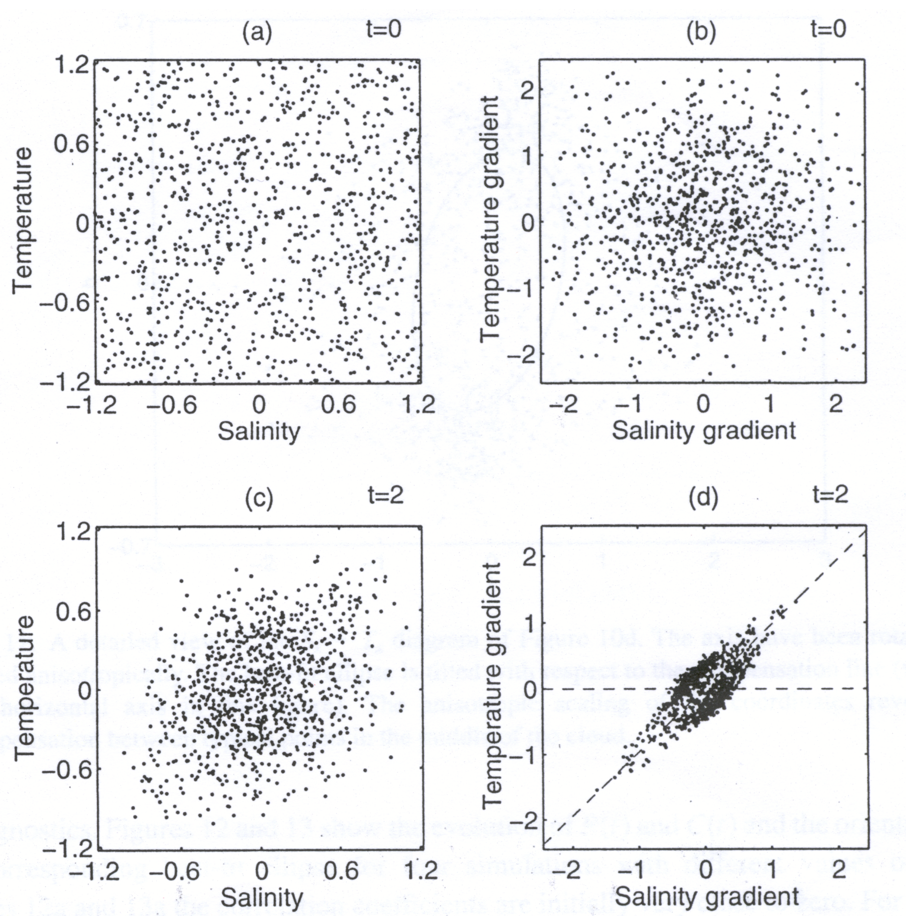

scatterplots at different times of heat and salt and their gradients

Independent variables: Buoyancy $B \equiv T - S$ and Spice $Q \equiv T + S$

Nonlinear diffusion equations

$$B_t = \gamma(B_x^3)_x, \quad Q_t = \gamma(B_x^2 Q_x)_x$$

Relevant related variables are the buoyancy gradient $h \equiv B_x$ and the spice gradient $j \equiv S_x$

$$h_t = \gamma(h^3)_{xx}, \quad j_t = \gamma(h_x^2 j)_{xx}$$

$h(t)$ active tracer, $j(t)$ passive tracer.

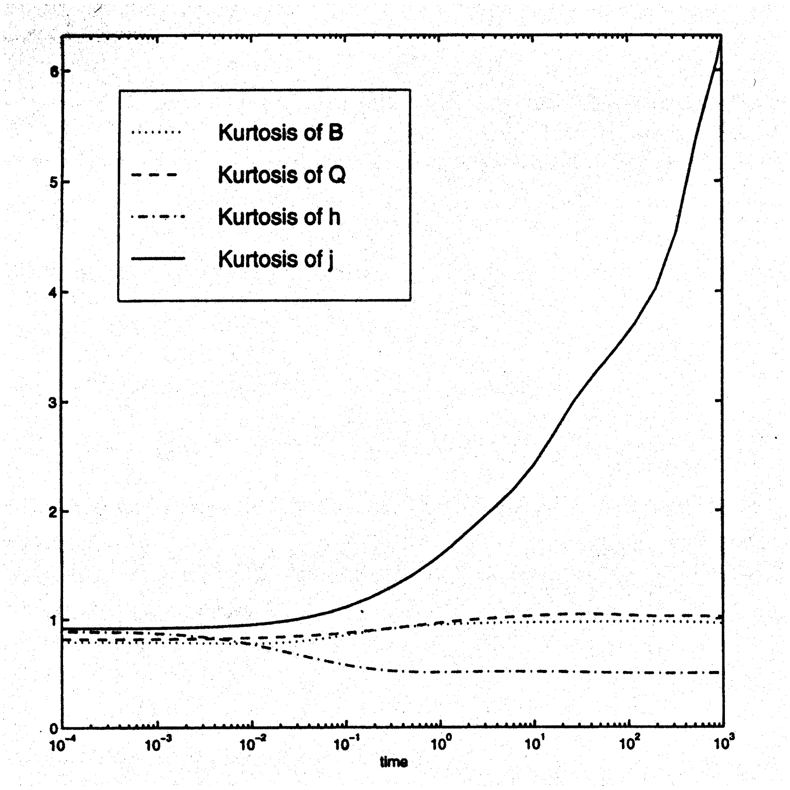

Time evolution of kurtosis of buoyancy and spice and of their gradients

Compensation is stronger between the gradients, T_x and S_x than between the fields T and S. This is expected to be a general consequence of nonlinear diffusion parameterizations in which the diffusivity increases with the horizontal buoyancy gradient

Creation of small-scale structure in spice is also expected to be a general property of this class of models

Three-dimensional stirring of thermohaline fronts

Klein, Tréguier and Hua, 1998 (KTH98)

In deeper layers than the Mixed Layer, experimental data also display abundant evidence of small-scale thermohaline features, of a few kilometers width, characterized by $\Delta\rho << |\alpha\Delta T|, |\beta\Delta S|$ (Roden, 1977, Ahran, 1990, Ahran and King, 1995).

Generic mechanisms (McVean and Woods, 1980)

- stirring by geostrophic eddies produces generically small scale fronts
- because of the thermal wind constraint, strong horizontally straining regions coincide spatially with vertical ageostrophic circulation, preventing small scales in density

Three-dimensional Quasi-geostrophic stirring

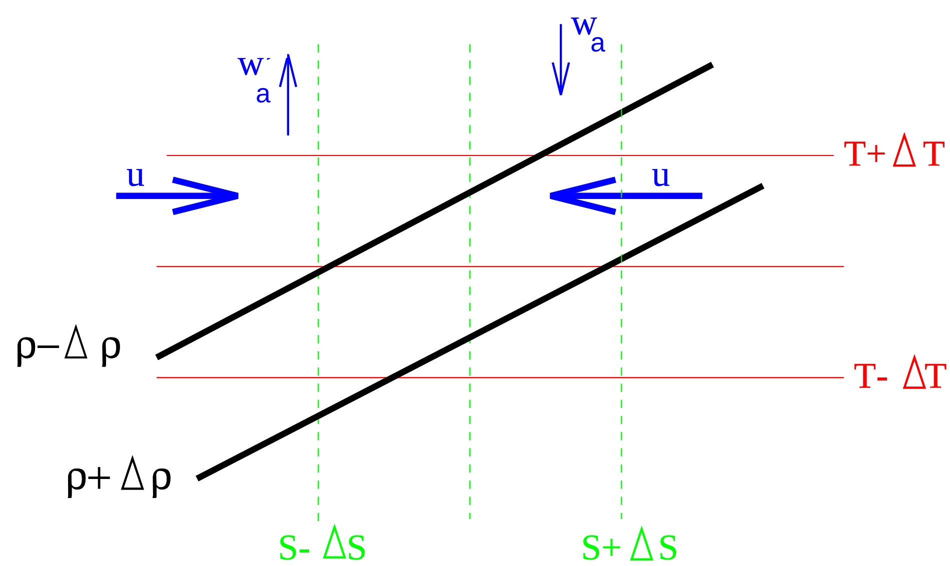

In this area of normal strain rate $(\partial u/\partial x < 0)$, the motions are nearly parallel to isopycnals cannot effectively increase density gradients. On the contrary such motions lead to an increase of gradients of temperature and salinity, which isopleths are inclined to the isopycnals.

$\boldsymbol{u}$ geostrophic velocities

w_a ageostrophic vertical velocity

For Quasi-geostrophic turbulence

- density ρ has large spatial scales because of the thermal wind constraint:

$$\partial_z \boldsymbol{u}_\perp = \frac{g}{\rho_0 f} \boldsymbol{\nabla}_H \rho$$

where $\boldsymbol{u}_\perp = \hat{\boldsymbol{z}} \times \boldsymbol{u}$ is at right angle to the geostrophic velocity.

Since the geostrophic velocity $\boldsymbol{u}$ (as well as $\partial_z \boldsymbol{u}_\perp$) has a horizontal wavenumber spectrum that is in K_H^{-3}, thermal wind balance implies that the density spectrum presents a horizontal wavenumber spectrum in K_H^{-5}, so that this steep spectrum law implies that in geostrophic turbulence, the density field is dominated by large spatial scales.

- On the other hand, both temperature T and salinity S behave like passive tracers fields, thus will have small spatial scales and their horizontal wavenumber spectrum that is in K_H^{-1}

Ageostrophic circulation in 2D and 3D

For a given tracer C the tracer gradient formation for strictly 2D flows is

$$\frac{D}{Dt}\,\boldsymbol{\nabla} C = -\boldsymbol{A}\,\boldsymbol{\nabla} C, \qquad \boldsymbol{A} = [\,\boldsymbol{\nabla}\boldsymbol{u}]^*,$$

with horizontal $\boldsymbol{u} = (u, v)$, $\frac{D}{Dt} \equiv \frac{\partial}{\partial t} + \boldsymbol{u}\cdot\ \boldsymbol{\nabla}$, $\boldsymbol{\nabla} = (\partial_x, \partial_y)$.

For a 3D Quasigeostrophic circulation,

$$\frac{D}{Dt}\,\boldsymbol{\nabla} C = -\boldsymbol{A}\,\boldsymbol{\nabla} C + \frac{\partial \overline{C}}{\partial z}\,\boldsymbol{\nabla} w_a$$

where $\frac{\partial \overline{C}}{\partial z}$ depends on the large-scale distribution of $\overline{C}$, and w_a is the vertical velocity (the subscript a denotes its ageostrophic character).

If we take $C = \rho$ in the above equation, together with the gradient of the LHS of the thermal wind constraint this leads to

$$\begin{aligned}
\frac{D}{Dt}\,\boldsymbol{\nabla}\rho &= -\overbrace{\boldsymbol{A}\ \boldsymbol{\nabla}\rho} &&+ \overbrace{\mathcal{S}\,\boldsymbol{\nabla} w_a} \\
\frac{D}{Dt}\partial_z \boldsymbol{u}_\perp &= +\underbrace{\boldsymbol{A}\ \partial_z \boldsymbol{u}_\perp}_{\text{nonlinear straining}} &&+ \underbrace{f\,\partial_z \boldsymbol{u}_a}_{\text{ageostrophic circulation}}
\end{aligned}$$

where $\mathcal{S} = \frac{N^2\rho}{g}$. The thermal wind constraint imposes

$$\frac{D}{Dt}\,\boldsymbol{\nabla}\rho - \frac{D}{Dt}\partial_z \boldsymbol{u}_\perp = 0$$

- nonlinear straining by geostrophic eddies tend to destroy the thermal wind balance.
- The ageostrophic circulation instantaneously restores the thermal wind balance. This ageostrophic vertical velocity enables the flow to remain along isopycnal surfaces and suppresses all the frontogenetical effects on ρ

The above arguments are first order in Lagrangian derivative, the dynamics involving second-order Lagrandian accelerations are elaborated in Hua, McWilliams and Klein, 1998

Numerical simulations of thermohaline stirring

KTH98 considered an idealized distribution such that the large-scale isotherms are horizontal and large-scale isohaline surfaces are vertical. Such a situation presents similar characteristics to the observational study of Ahran and King, 1995 in the Northeast Atlantic, where a large-scale thermohaline front separates the Mediterranean Water from the Intermediate Artic Water. Such orthogonal large-scale forcings highlight the dynamical processes which come into play in the formation of thermohaline compensated fronts.

Their equations obey

$$\frac{DS}{Dt} + v\frac{\partial \overline{S}}{\partial y} = 0$$
$$\frac{DT}{Dt} + w_a\frac{\partial \overline{T}}{\partial z} = 0$$

and by construction their differences is identical to the equation for density.

The quasi-geostrophic flow field obeys the usual PV conservation equation

$$\frac{Dq}{Dt} + v\frac{\partial \overline{q}}{\partial y} = D$$

$$\begin{aligned} q &= \boldsymbol{\nabla}^2\phi + \frac{\partial}{\partial z}\left(\frac{f^2}{N^2}\frac{\partial \phi}{\partial z}\right) \\ \frac{\partial q}{\partial y} &= \beta - \frac{\partial}{\partial z}\left(\frac{f^2}{N^2}\frac{\partial \overline{U}}{\partial z}\right) \end{aligned}$$

(a) **density**

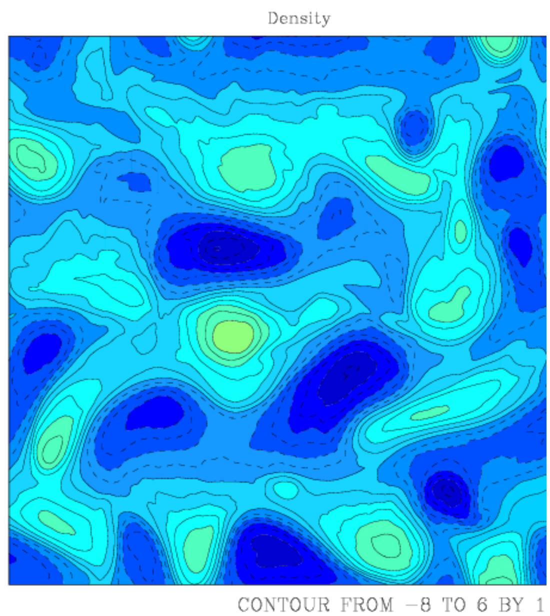

(b) **salinity and temperature**

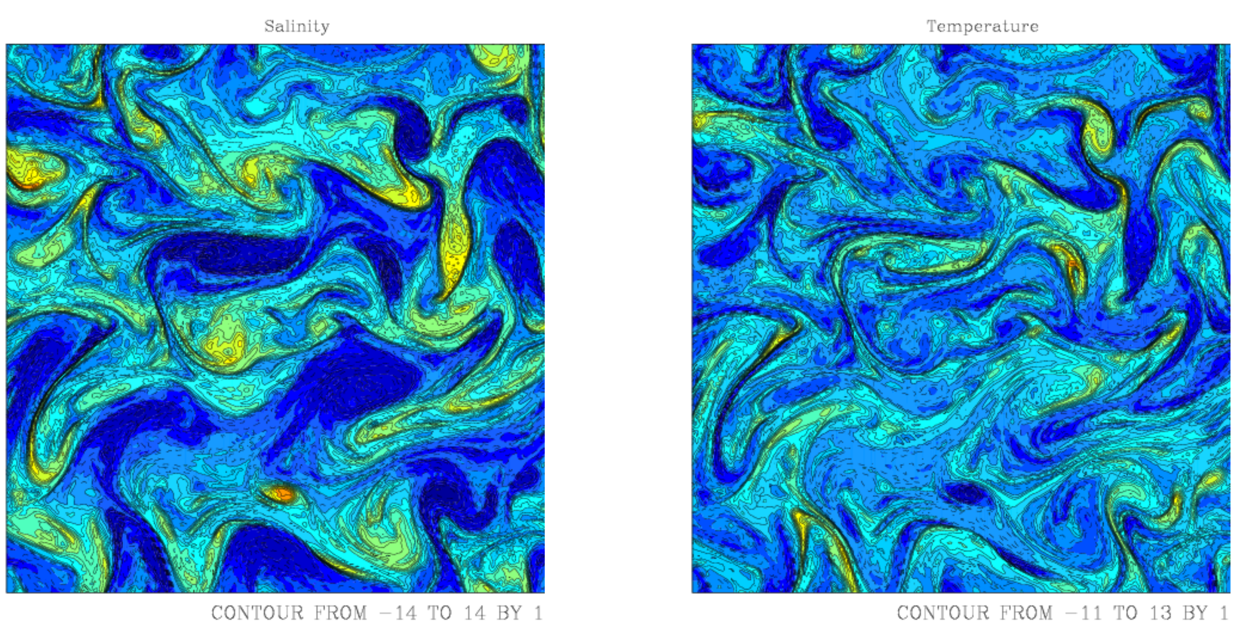

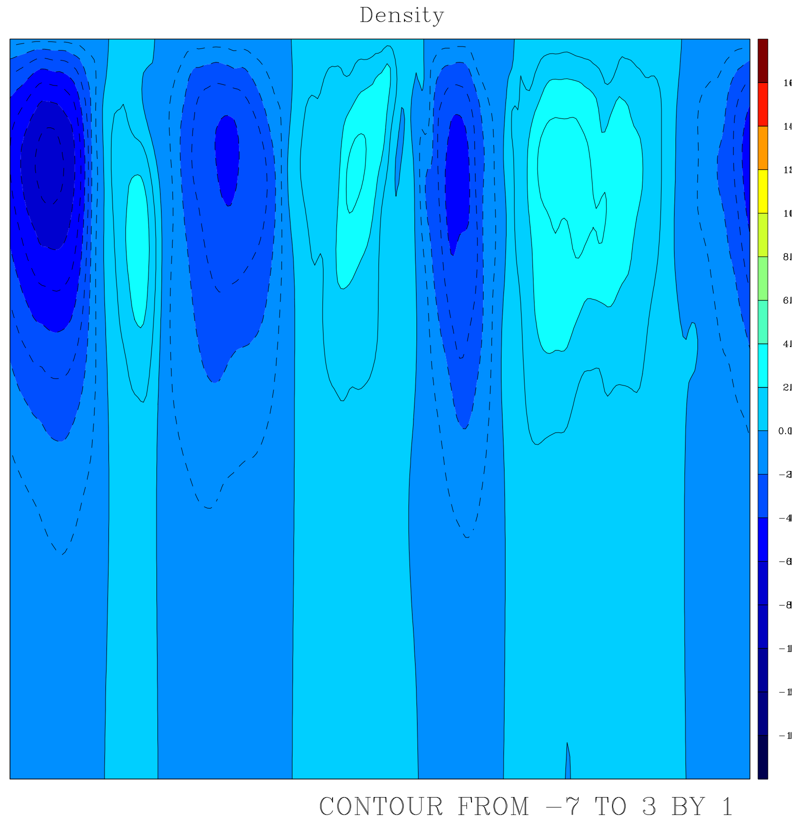

Density field

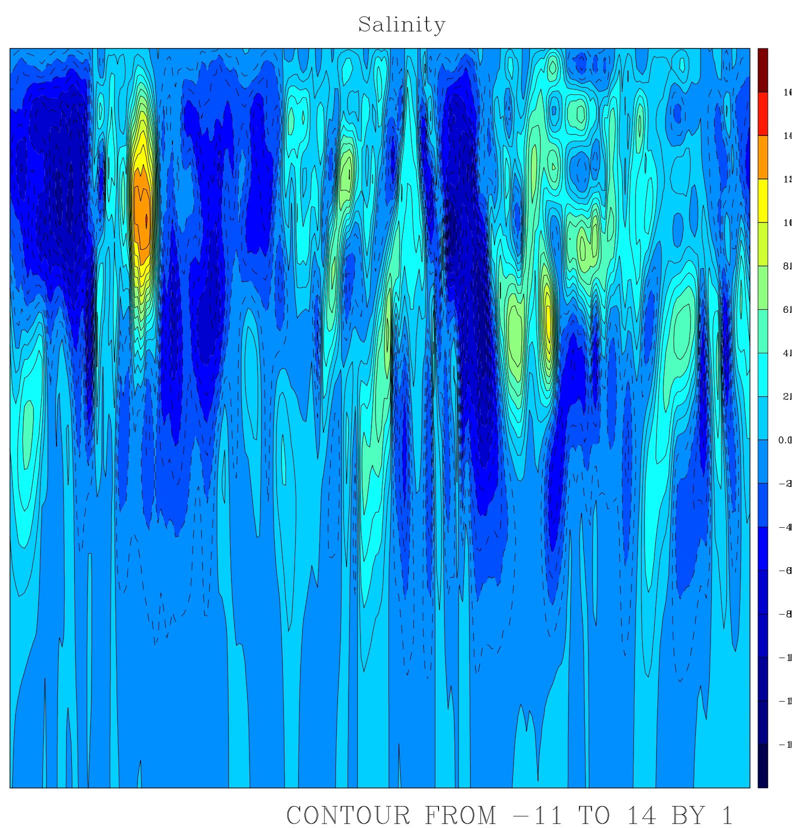

Salinity field

Okubo-Weiss

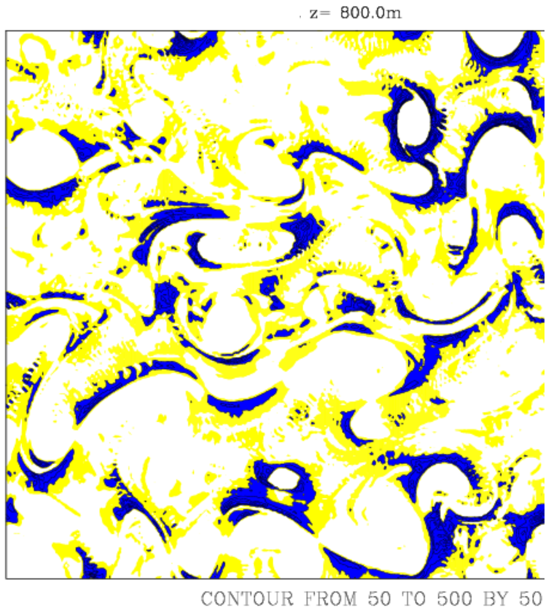

Strain-acceleration eigenvalue

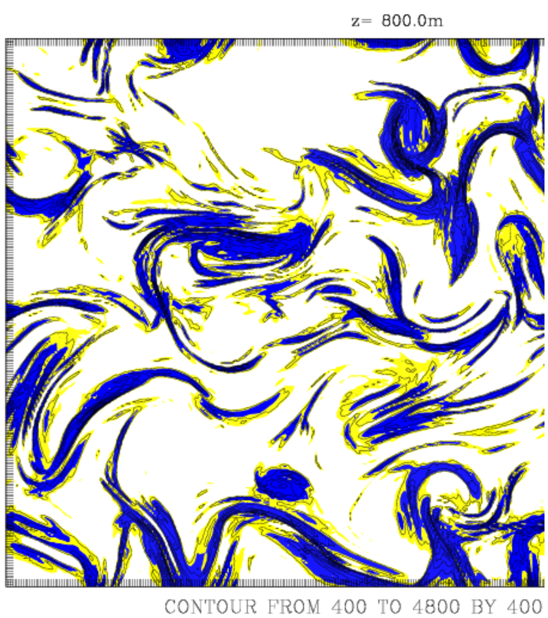

Long-range influence in space, which is larger-amplitude.
Creation of partially-compensated thermohaline fronts

SUMMARY

- Spice T+S generally observed to present higher levels of variance than density T-S

- Mixed layer**: nonlinear diffusion** induces a **selective decay** for randomly generated initial tracer perturbations

- Subsurface layers: **geostrophic stirring along density surfaces** will cause a **selective generation** of T and S gradients

- **Convection areas**: both upright plume convection and slant-wise baroclinic eddy can generate small scale variance in spice (Legg et al. 2000)

-

References :

Arhan, M. 1990. The North Atlantic Current and Subartic Intermediate Water. J. Mar. Res., 48, 109-144.

Arhan, M. 1995. Lateral mixing of the Mediterranean Water in the eastern North Atlantic, J. Mar. Res, 53, 865-895.

Ferrari R and W. R. Young 1997. On the development of thermohaline correlations as a result of nonlinear diffusive parameterisations. J. Mar. Res., 55, 1069-1101.

Iselin, 1939. Trans. Am. Geophys. Union, 20, 414.

Klein, P., A.M. Tréguier and B.L. Hua. Three-dimensional stirring of thermohaline fronts. J. Mar. Res., 56, 589-612.

Legg S., J. C. McWilliams, 2000. Temperature and salinity variability in heterogeneous oceanic convection. J. Phys. Oceanog., 30, 1188-1206.

Lilly, J. M., P.B. Rhines, M. Visbeck, R. Davis, J.R. Lazier, F. Schott and D. Farmer, 1999. Observing deep convection in the Labrador Sea during winter 1994-1995. J. Phys. Oceanog., 29, 2065-2098

McVean, M.K. and J.D. Woods, 1980. Redistribution of scalars during upper frontogenesis: a numerical model. Quart. J. Roy. Soc. Meteor. Soc., 106, 293-311.

Hua, B.L., J McWilliams and P. Klein, 1998. Lagrangian accelerations in geostrophic turbulence. J. Fluid Mech. ., 366, 87-108.

Okubo, A. 1970. Horizontal dispersion of floatable particles in the vicinity of velocity singularities such as convergence, Deep Sea Res, 17, 445-454.

Roden, G. I. 1977. Oceanic Subartic fronts of the central Pacific: structure and response to atmospheric forcing. J. Phys. Oceanog., 7, 761-778.

Rudnick D.L. and R. Ferrari, 1999. Compensation of horizontal temperature and salinity gradients in the ocean mixed layer. Science, 283, 526-529.

Weiss, J., 1991. The dynamics of enstrophy transfer in two-dimensional hydrodynamics, Physica D, 48, 273-294.